Sparse Time Series Sampling for Recovery of Behind-the-Meter Inverter Control Models

Samuel Talkington, Santiago Grijalva
School of Electrical and Computer Engineering
Georgia Institute of Technology
Atlanta, GA, USA
{stalkington3,sgrijalva6}@gatech.edu

Matthew J. Reno
Electric Power Systems Research
Sandia National Laboratories
Albuquerque, NM, USA
mjreno@sandia.gov

***Abstract*—Incorrect modeling of control characteristics for inverter-based resources (IBRs) can affect the accuracy of electric power system studies. In many distribution system contexts, the control settings for behind-the-meter (BTM) IBRs are unknown. This paper presents an efficient method for selecting a small number of time series samples from net load meter data that can be used for reconstructing or classifying the control settings of BTM IBRs. Sparse approximation techniques are used to select the time series samples that cause the inversion of a matrix of candidate responses to be as well-conditioned as possible. We verify these methods on 451 actual advanced metering infrastructure (AMI) datasets from loads with BTM IBRs. Selecting 60 15-minute granularity time series samples, we recover BTM control characteristics with a mean error less than 0.2 kVAR.**

***Index Terms*—Advanced inverters, sensor placement, voltage regulation, convex optimization, sparse representation**

I. Introduction

Behind-the-meter (BTM) inverter-based resources (IBRs) are poised to have a large impact on distribution grid infrastructure and on the methods used for electric power system studies. In general, the diversity [1] of inverter control settings can make it difficult to accurately determine the impact that IBRs may have on a system. In this paper, a technique is developed to expose unknown IBR control models from *net load* advanced metering infrastructure (AMI) data. This is achieved by finding a sparse representation for the reactive power time series in a basis of candidate control model responses.

The presented method is based on the results of [2]–[4], which develop signal processing techniques for stable recovery of a signal through a very small number of salient samples that may be corrupted. Due to the influence of noise and the *native* load signal, it is difficult to determine the impact of a BTM IBR from net load AMI data using conventional estimation methods. However, some samples are occasionally composed mostly of contributions of the IBR. Extracting these samples provides information about the IBR control "model" or "curve" $\phi_\Theta(x_t)$. The structure of this control model is defined by a vector of parameters $\Theta \in \mathbb{R}^k$. For example, Θ could be the $k/2$ "knots" of a Volt-VAR curve of the form $(V_1, Q_1), \ldots, (V_4, Q_4)$, as shown in Fig. 1, or the slope of a fixed power factor line in the complex plane. The control input x_t is a time series measurement at the load at index $t \in [\![1, m]\!]$ (e.g., the voltage, in the case of Volt-VAR).

The contribution of this work is a method to automatically select the samples $\gamma \subset \{1, \ldots, m\}$ of historical AMI measurements that are optimal for identifying a BTM control model, where the number of these measurements, $|\gamma| \triangleq p$, is much smaller than m. The samples selected are ones when the IBR's contribution dominates the AMI signal, enabling the underlying control model to be reconstructed or classified. The reconstructed control model can then be used to disaggregate the IBR contribution from the net load signal.

II. Background

Recent works have shown that it is possible to recover reactive power control settings of IBRs from AMI signals, with data input requirements ranging from voltage magnitudes [5] to net load data [6]. When using the net load reactive power measurements directly as in [6], manual tuning of a filter is required in order to disaggregate the native and IBR reactive power signals. In contrast, this paper is a generalization of these methods. Specifically, this paper provides an entirely unsupervised method to select the most well-conditioned time series samples for reconstructing these settings based on the QR decomposition. This method is robust to the presence of heavy corruption from the native load signal, and removes the need for manual tuning, as used in [6].

A. Net Load Measurements

Let $\mathcal{N}$ be the set of all slack and PQ buses in a radial distribution network. We consider net load voltage, active, and reactive power time series measurements over a total time horizon m from an AMI sensor at a bus $l \in \mathcal{N}$:

$$\mathcal{D}_l = (\mathbf{v}, \mathbf{p}^{net}, \mathbf{q}^{net}) = \{(v_t, p_t^{net}, q_t^{net})\}_{t=1}^m \tag{1}$$

Submitted to the thirteenth Conference on Innovative Smart Grid Technologies (ISGT 2022), North America.

This work has been partially supported by the U.S. Department of Energy's Office of Energy Efficiency and Renewable Energy (EERE) under Solar Energy Technologies Office (SETO) Agreement Number 34226. Sandia National Laboratories is a multi-mission laboratory managed and operated by National Technology and Engineering Solutions of Sandia, LLC., a wholly owned subsidiary of Honeywell International, Inc., for the U.S. Department of Energy's National Nuclear Security Administration under contract DE-NA0003525. This paper describes objective technical results and analysis. Any subjective views or opinions that might be expressed in the paper do not necessarily represent the views of the U.S. Department of Energy or the United States Government.

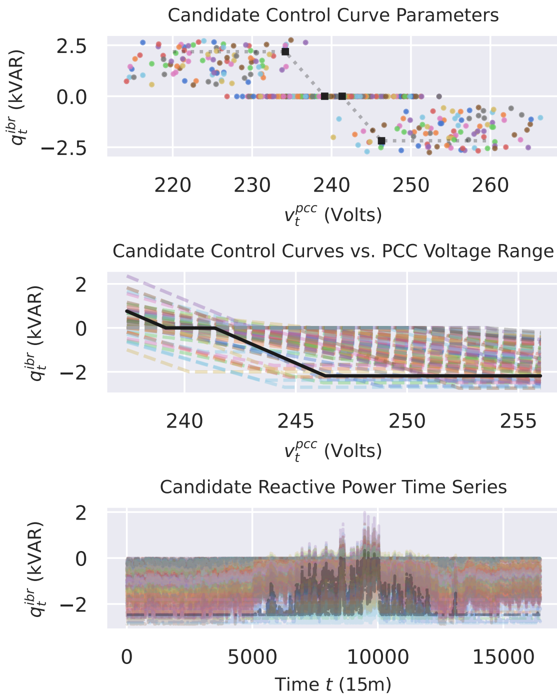

Figure 1. From top to bottom, with ground truths shown in black: a) a set of candidate Volt-VAR control parameter vectors b) candidate control curves corresponding to the candidate parameter vectors c) candidate reactive power time series responses corresponding to the candidate control curves.

Remark (Sign Convention)**.** *To make the notation more intuitive, we adopt the convention that injections from a node into the distribution system are positive and flows from the distribution system into the load through the AMI are negative.*

We assume that $\mathbf{q}^{net} \in \mathbb{R}^m$ is measured at a bus l with a BTM IBR, and define this signal as the sum of the IBR contribution and the "native" load contribution:

$$\mathbf{q}^{net} \triangleq \mathbf{q}^{ibr} + \mathbf{q}^{nat} \tag{2}$$

At time t, the contribution of the IBR to the AMI-observed net reactive power signal can be characterized by the parameter vector $\Theta \in \mathbb{R}^k$, as shown in Fig. 1.

$$\mathbf{q}^{ibr} = [\phi_\Theta(x_1), \ldots, \phi_\Theta(x_m)]^T \in \mathbb{R}^m \tag{3}$$

B. IBR Control Basis Functions

Consider a BTM IBR whose reactive power injection is controlled according to $q_t^{ibr} = \phi_\Theta(x_t)$, where x_t is the controller input derived from the AMI time series.

For power factor control, this is typically the IBR active power generation. The reactive power contribution of the IBR is determined by a sensitivity parameter $\frac{\Delta Q}{\Delta P}$, which defines a linear function in the complex plane fixed at the origin.

$$\phi\left(\tilde{p}_t^{ibr}; \frac{\Delta Q}{\Delta P}\right) = \frac{\Delta Q}{\Delta P}\left(\tilde{p}_t^{ibr}\right) \tag{4}$$

Fixed power factor control requires the input $\tilde{p}_t^{ibr}$ to be the output of a disaggregation algorithm to estimate the contribution of $\mathbf{p}^{ibr}$ to the net power signal in (1). There are many methods to achieve this, such as [7]–[9] and others.

For autonomous Volt-VAR control, the control input is the PCC voltage, assumed to be measured directly by the AMI [1]. This control model can be written as (5).

$$\phi_\Theta(v_t) = \begin{cases} Q_1 & v_t \le V_1 \\ (v_t - V_1)\frac{Q_2 - Q_1}{V_2 - V_1} + Q_1 & V_1 < v_t < V_2 \\ 0 & V_2 \le v_t \le V_3 \\ (v_t - V_3)\frac{Q_4 - Q_3}{V_4 - V_3} + Q_3 & V_3 \le v_t \le V_4 \\ Q_4 & v_t > V_4 \end{cases} \tag{5}$$

C. Compressed Sensing and Sparse Representation

The signal processing techniques of compressed sensing and sparse representation show that real-world signals are often able to be reconstructed through a very small number of measurements [10]–[12]. This technique is based on the fact that signals are often sparse in a basis representation $\mathbf{\Psi} \in \mathbb{R}^{m \times n}$. A signal $\mathbf{x} \in \mathbb{R}^m$ is known as being k-sparse in this basis if it can be written as a linear system of equations defined by $\mathbf{\Psi}$ and a vector $\mathbf{s} \in \mathbb{R}^n$ with k non-zero entries:

$$\mathbf{x} = \mathbf{\Psi}\mathbf{s} \tag{6}$$

If $k \ll n$ it is possible to reconstruct $\mathbf{x}$ with $\mathcal{O}(k \log(n/k))$ random measurements. Depending on the randomness of the measurements and the nature of the basis, this reconstruction can be near-exact [10], [12], or even exact [11]. Most work in this area is focused on generalized basis representations, such as Fourier or wavelet coefficients. Computing these transforms can be computationally expensive.

III. Sparse Sampling of AMI Time Series

The problem of disaggregating BTM IBR contributions from net load reactive power signals can be solved by using a low-rank basis in a similar form to (6). This relates to other works such as [8], [9] which have also utilized sparse representation methods in the context of estimating active power contributions.

The linear system (6) can be adapted to a tailored basis $\mathbf{\Psi}_r \in \mathbb{R}^{m \times r}$ found through the singular value decomposition (SVD), which we develop in the next section, or another matrix decomposition method.

A. Low-Rank Representation of AMI Data

Referencing results in sparse sensing such as [2], our problem can be understood as finding an optimal sparse measurement matrix $\mathbf{C} \in \mathbb{R}^{p \times m}$ which is then used to minimize the condition number of the linear system (7):

$$\mathbf{q}^{net} = \mathbf{C}\mathbf{\Psi}_\mathbf{r}\mathbf{s} = \boldsymbol{\theta}\mathbf{s} \tag{7}$$

which is given as the ratio of the maximum and minimum singular values of the matrix.

$$\boldsymbol{\theta}(\mathbf{s} + \epsilon) = \sigma_{min}\mathbf{s} + \sigma_{max}\epsilon \tag{8}$$

This causes the inversion of the matrix $\boldsymbol{\theta}$ to be well-conditioned and identifies the low-rank coefficients in the noisy time series $\mathbf{q}^{net}$. This allows us to achieve the goal of selecting salient time series measurement samples $\boldsymbol{\gamma} \subset [\![1, m]\!]$ that can be used to best approximate the high dimensional state of the controller output (3). Specifically, we want $\boldsymbol{\gamma}$ to be the subset of the time series that is primarily composed of the controller output behavior.

By using the physical definitions of control curves such as (5) or (4), we can form a basis of candidate control responses $\Psi \in \mathbb{R}^{m \times n}$:

$$\Psi = \begin{bmatrix} \vdots & \vdots & & \vdots & \vdots \\ \phi_{\Theta_1}(\mathbf{x}) & \phi_{\Theta_2}(\mathbf{x}) & \dots & \phi_{\Theta_{n-1}}(\mathbf{x}) & \phi_{\Theta_n}(\mathbf{x}) \\ \vdots & \vdots & & \vdots & \vdots \end{bmatrix} \quad (9)$$

and augment this basis to sample the optimal measurements for reconstructing or classifying the control model. A control model reconstructed with these samples will allow $\mathbf{q}^{ibr}$ and $\mathbf{q}^{nat}$ to be disaggregated in a data-driven manner, without access to the distribution system model.

The singular value decomposition (SVD) for any complex valued matrix $\boldsymbol{\Psi} \in \mathbb{C}^{m \times n}$ is given as (10), where $\mathbf{U} \in \mathbb{C}^{m \times m}$, $\mathbf{V} \in \mathbb{C}^{n \times n}$ are orthonormal matrices, $\boldsymbol{\Sigma} \in \mathbb{R}^{m \times n}$ is a diagonal matrix of singular values, and $*$ is the complex conjugate transpose.

$$\boldsymbol{\Psi} = \mathbf{U}\boldsymbol{\Sigma}\mathbf{V}^* \quad (10)$$

Using (10), we can form a low-rank basis $\Psi_r \in \mathbb{R}^{m \times r}$ of control curves to define a new coordinate system.

Theorem 1 (Low-dimensional control curve basis)**.** *The Eckart-Young Theorem [13] establishes that the rank-r matrix that optimally approximates $\boldsymbol{\Psi}$ is the solution to the optimization problem (11):*

$$\boldsymbol{\Psi}_r = \underset{\tilde{\boldsymbol{\Psi}}:rank(\tilde{\boldsymbol{\Psi}})=r}{\arg\min} ||\boldsymbol{\Psi} - \tilde{\boldsymbol{\Psi}}||_F = \tilde{\mathbf{U}}\tilde{\boldsymbol{\Sigma}}\tilde{\mathbf{V}}^* \quad (11)$$

Where $||.||_F$ is the Frobenius norm, $\tilde{\boldsymbol{\Sigma}}$ is the first $r \times r$ submatrix of $\boldsymbol{\Sigma}$, and $\tilde{\mathbf{U}}, \tilde{\mathbf{V}}^*$ are the first r columns of $\mathbf{U}, \mathbf{V}$

The Eckart-Young Theorem gives a low-rank representation basis $\boldsymbol{\Psi}_r$ onto which we project the net load signal $\mathbf{q}^{net}$ [2], [3]. The notion of sparsity in a basis of orthogonally decomposed test signals has proven effective for various signal reconstruction tasks in many different domains, including electric power system studies [9], [14].

To select the optimal samples for identifying the control settings, we seek a linear measurement operator $\mathbf{C} \in \mathbb{R}^{p \times m}$ which is used to find $p \ll m$ optimal measurement samples, denoted as $\tilde{\mathbf{q}}^{net} \in \mathbb{R}^p$:

$$\tilde{\mathbf{q}}^{net} = \mathbf{C}\mathbf{x} = \mathbf{C}\boldsymbol{\Psi}_r\mathbf{s} \quad (12)$$

B. Reconstructing Control Settings

Suppose that a load with a BTM distributed generator is under study and assume that the presence of an IBR is already determined.

As shown in Fig. 2, We construct the rank-r tailored basis of test signals $\boldsymbol{\Psi}_r \in \mathbb{R}^{m \times r}$ using the SVD. The original design

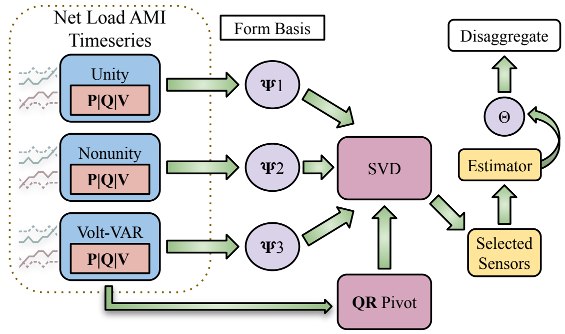

Figure 2. Proposed control curve reconstruction scheme showing novel sparse sampling technique. Once the unknown control type is determined, the AMI data is evaluated over the family of candidate control curves to form a basis. The cost-constrained QR factorization is used to select the best samples for well-conditioned reconstruction in the chosen basis.

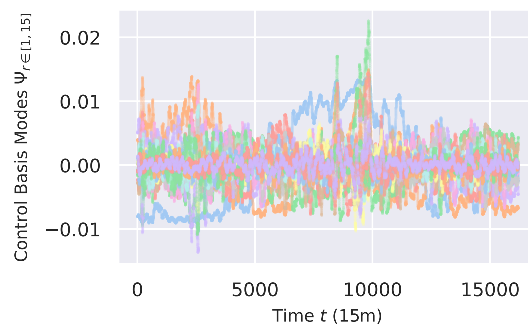

Figure 3. $r = 15$ SVD basis modes for IBR reactive power time series found using (11) with a Volt-VAR curve family as in (13). Daily rolling average.

matrix $\boldsymbol{\Psi}$ is formed by evaluating with the AMI datab a family $\mathcal{F} = \{\phi_{\Theta_1}, \dots, \phi_{\Theta_n}\}$ of n candidate control curves:

$$\phi_{\Theta_i} : \mathbb{R}^m \mapsto \mathbb{R}^m \ i \in [\![1, m]\!] \quad (13)$$

We define the feasible set $\mathcal{K}$ as the set of all control parameters Θ that satisfy the constraints for one of u control types, e.g., the set of all valid Volt-VAR knots in the IEEE 1547-2018 standard, or the range of valid fixed unity or nonunity power factor sensitivities.

$$\mathcal{K} = \{\Theta : \mathbf{A}_1\Theta \leq \mathbf{b}_1 \cup, \dots, \cup \mathbf{A}_u\Theta \leq \mathbf{b}_u\} \quad (14)$$

The basis $\boldsymbol{\Psi} \in \mathbb{R}^{m \times n}$ of candidate control signals is evaluated using the available AMI time series according to (9). Assume that $\Theta_i \in \mathcal{K}\ \forall i \in [\![1, n]\!]$. For example, $\mathcal{K}$ could be a set of candidate Volt-VAR curve parameters in Fig. 1.

Using (12), our problem can then be understood as finding the sparsest measurement matrix $\mathbf{C} \in \mathbb{R}^{p \times m}$, where $p \ll m$, that allows us to recover the high dimensional state approximately from a linear projection of the form of (12). A summary of this general reconstruction task is shown in Fig. 2.

Suppose that we have confidence that a load has a BTM IBR using Volt-VAR. In such an instance, $\boldsymbol{\Psi}_r \in \mathbb{R}^{m \times r}$ can be a matrix whose columns are orthogonal "eigen-volt-

VAR" response curves that form a new coordinate system for representing the measurements, as shown in Fig. 3.

IV. Reconstruction from Sparse Samples

This results in a linear system which represents p elements of the net load AMI measurements being selected through the use of $\boldsymbol{\Psi_r}\mathbf{s}$. The inverse problem can be written in terms of the Moore-Penrose pseudoinverse as:

$$\hat{\mathbf{s}} = \boldsymbol{\theta}^{\dagger}\mathbf{q}^{net} = (\mathbf{C}\boldsymbol{\Psi}_r)^{\dagger}\mathbf{q}^{net} \tag{15}$$

so, we can write the reconstruction as:

$$\hat{\mathbf{x}} = \boldsymbol{\Psi}_r\hat{\mathbf{s}} = \begin{cases} (\mathbf{C}\boldsymbol{\Psi}_r)^{-1}\mathbf{q}^{net} & \text{if } p = r \\ (\mathbf{C}\boldsymbol{\Psi}_r)^{\dagger}\mathbf{q}^{net} & \text{if } p > r \end{cases} \tag{16}$$

A. Relationship to the $\mathbf{QR}$ Factorization

The QR factorization decomposes a rectangular matrix $\mathbf{A} \in \mathbb{R}^{m\times n}$ into the product of a unitary matrix $\mathbf{Q}$ and upper-triangular matrix $\mathbf{R}$ and is ubiquitous in linear least squares and inverse problems.

Referencing [2], [4], [15], the optimal sensors $\boldsymbol{\gamma}$, encoded through $\mathbf{C}$ can be found with the QR factorization, with column pivoting of $\boldsymbol{\Psi}_r^T$:

$$\boldsymbol{\Psi}_r^T\mathbf{C}^T = \mathbf{QR} \tag{17}$$

For the oversampled case where $p > r$, which is the case in our experiments, we have:

$$(\boldsymbol{\Psi}_r\boldsymbol{\Psi}_r^T)\mathbf{C}^T = \mathbf{QR} \tag{18}$$

In summary, the optimal time series sampling problem can be related to the QR decomposition in the form of (19).

$$\begin{cases} \boldsymbol{\Psi}_r^T\mathbf{C}^T = \mathbf{QR} & p = r \\ (\boldsymbol{\Psi}_r\boldsymbol{\Psi}_r^T)\mathbf{C}^T = \mathbf{QR} & p > r \end{cases} \tag{19}$$

Applying the cost-constraint QR factorization algorithm in [4], [16], cost values equal to the net real power are assigned to weight the samples.

What this does is encourage the selection of the samples where $p_t^{net} < 0$, which is intuitive, as the inverter will likely be regulating voltage when the BTM IBR causes the load to be a net generator. This causes the $\mathbf{QR}$ pivoting algorithm to balance mathematical factorization error with respecting physical intuition. In our experiments, this algorithm configuration results in the selection of samples that are mostly composed of IBR contributions; approximating the control model response.

B. Identifying Control Models

After selecting the p optimal time series samples for reconstructing in the selected basis utilizing the $\mathbf{QR}$ pivot strategy, reconstructing the control curve then boils down to an estimation problem. The parameter vector $\hat{\Theta}$ that best approximates the samples while satisfying the feasibility constraints (14) in the least-squares sense is:

$$\hat{\Theta} = \underset{\Theta\in\mathcal{K}}{\arg\min} \sum_{m=1}^{p} |q_m^{net} - \phi_{\Theta}(v_m)|^2 \tag{20}$$

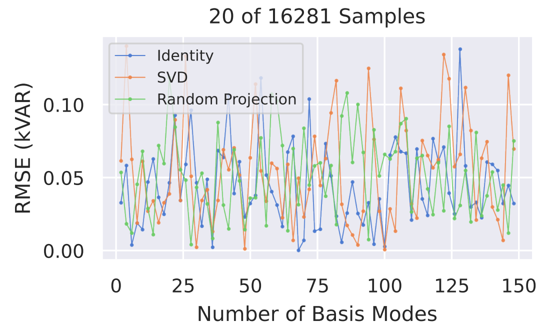

Figure 4. Reconstruction error for a single load with unknown Volt-VAR control settings as a function of the number of SVD basis modes r.

V. Experiments

Volt-VAR control has shown promise for at-scale integration of inverter-based resources due to its voltage regulation capabilities with superior performance in comparison to fixed power factor control. For this reason and for brevity, we validate the method by showing reconstruction performance for these curves. Much of the sparse sensor placement theory has been implemented in Python [16], which is useful for conducting the experiments in this section.

A. Varying the Basis and Number of Basis Modes

The basis $\boldsymbol{\Psi}_r$ need not be the solution to (11) but can be any matrix derived from $\mathcal{D}_l$, such as random projections of the rows of $\mathcal{D}_l$ or simply an identity matrix multiplied by the multivariate timeseries formed by $\mathcal{D}_l$. We consider all of these different representations in Fig. 4. We reconstruct the control model using (20) and calculate the root-mean-square error (RMSE) of the estimated reactive power injections for the IBR throughout the year, where all perform with RMSE values distributed between 0 to 0.15 kVAR for basis modes $r \in [\![1, 150]\!]$. Considering a fixed number of samples $p = 20$ to be selected out 16281 possible samples, the variance of the model can be evaluated by iterating over a range of values of r, comparing the reconstruction accuracy as shown in Fig. 4.

B. Large Scale Testing

We evaluate the proposed method on 451 actual load datasets with a BTM IBR. The variation of control parameters is shown in Fig. 1.a. These loads have a single BTM control model; handling loads with multiple BTM models remain an opportunity for future work. We choose $p = 60$ sensors using $r = 15$ basis modes, and the sensors are selected according to the cost-constrained $\mathbf{QR}$ pivot. These parameters were chosen through a 10-fold cross validation. Across all loads tested, we reconstruct the high-dimensional BTM reactive power state with an average RMSE of 0.1937 kVAR. The empirical distribution of the RMSE values is shown in Fig. 5.

The method selects a small number of samples to provide accurate reconstruction of the inverter control settings, with sole reliance on relatively affordable QR factorization and least squares computations. An example of this is shown in Fig. 6.

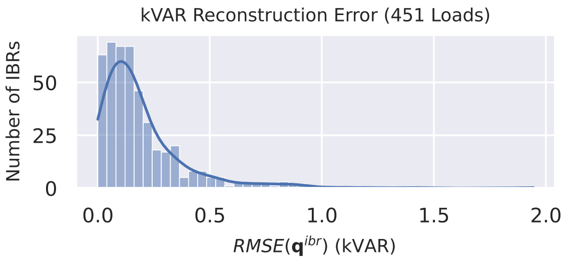

Figure 5. Empirical histogram of RMSE values for the 451 loads evaluated. For all experiments, the number of samples selected is $p = 60$ and the number SVD basis modes is $r = 15$.

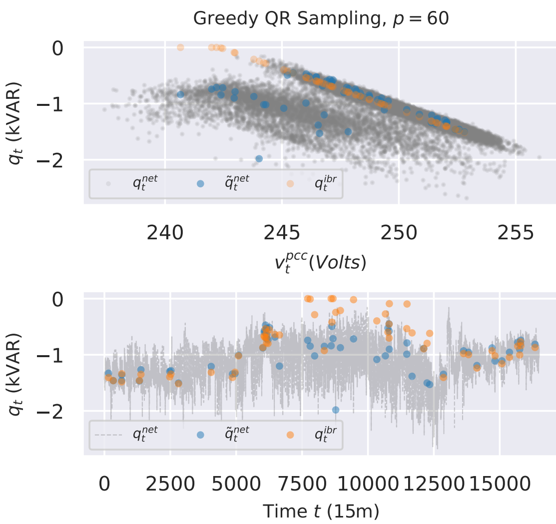

Figure 6. Sparse sampling for $p = 60$ measurements with the cost constrained QR problem. By color: (orange) true unobservable IBR reactive power measurements (blue) sampled net reactive power measurements (grey) net reactive power measurements. From top to bottom: (a) control curve reconstruction (b) time series sampling.

If ϕ_Θ is a function of a signal that is observable by the AMI, e.g., Volt-VAR or Volt-Watt, the user can disaggregate the corresponding net active or reactive power signal observed in (2) at any other time the controller is active—after $\hat{\Theta}$ is found using (20) or another method of choice.

$$\hat{y}_t^{nat} = y_t^{net} - \phi_{\hat{\Theta}}(x_t) \quad \forall t \in [\![1, m]\!] \tag{21}$$

where x, y are the inputs and outputs of ϕ_Θ respectively.

VI. Conclusion

We have presented an efficient method for selecting a small number of time series measurement samples from historical AMI data that are optimal for identifying an unknown BTM IBR control model. The method allows the user to avoid the influence of noise and the native demand signal within the net AMI data stream. These samples are selected by making a matrix of candidate responses as well conditioned as possible. The underlying control model can then be reconstructed or classified with the chosen samples without need for training data or a physical model of the network.

Acknowledgment

The authors would like to thank Logan Blakely for insightful conversations and Joseph Azzolini for sharing some of the data used in the project behind this paper.

References

[1] "IEEE Standard for Interconnection and Interoperability of Distributed Energy Resources with Associated Electric Power Systems Interfaces," *IEEE Std. 1547-2018*, pp. 1–138, 2018.

[2] K. Manohar, B. W. Brunton, J. N. Kutz, and S. L. Brunton, "Data-driven sparse sensor placement for reconstruction: Demonstrating the benefits of exploiting known patterns," *IEEE Control Systems Magazine*, vol. 38, no. 3, pp. 63–86, 2018.

[3] B. W. Brunton, S. L. Brunton, J. L. Proctor, and J. N. Kutz, "Sparse Sensor Placement Optimization for Classification," *SIAM Journal on Applied Mathematics*, vol. 76, no. 5, pp. 2099–2122, Jan. 2016, publisher: Society for Industrial and Applied Mathematics. [Online]. Available: https://epubs.siam.org/doi/abs/10.1137/15M1036713

[4] E. Clark, T. Askham, S. L. Brunton, and J. Nathan Kutz, "Greedy Sensor Placement With Cost Constraints," *IEEE Sensors Journal*, vol. 19, no. 7, pp. 2642–2656, Apr. 2019.

[5] S. Talkington, S. Grijalva, and M. J. Reno, "Power Factor Estimation of Distributed Energy Resources Using Voltage Magnitude Measurements," *Journal of Modern Power Systems and Clean Energy*, vol. 9, no. 4, pp. 859–869, 2021.

[6] S. Talkington, S. Grijalva, M. J. Reno, and J. Azzolini, "Recovering Power Factor Control Settings of Solar PV Inverters from Net Load Data," to appear in The 53rd North American Power Symposium.

[7] E. C. Kara, C. M. Roberts, M. Tabone, L. Alvarez, D. S. Callaway, and E. M. Stewart, "Disaggregating solar generation from feeder-level measurements," *Sustainable Energy, Grids and Networks*, vol. 13, pp. 112–121, Mar. 2018. [Online]. Available: https://www.sciencedirect.com/science/article/pii/S2352467717301169

[8] P. Li, B. Zhang, Y. Weng, and R. Rajagopal, "A Sparse Linear Model and Significance Test for Individual Consumption Prediction," *IEEE Transactions on Power Systems*, vol. 32, no. 6, pp. 4489–4500, Nov. 2017.

[9] S. Lin and H. Zhu, "Enhancing the Spatio-Temporal Observability of Grid-Edge Resources in Distribution Grids," *IEEE Transactions on Smart Grid*, vol. 12, no. 6, pp. 5434–5443, Nov. 2021, conference Name: IEEE Transactions on Smart Grid.

[10] E. Candes and T. Tao, "Near Optimal Signal Recovery From Random Projections: Universal Encoding Strategies?" *arXiv:math/0410542*, Apr. 2006.

[11] E. Candes, J. Romberg, and T. Tao, "Robust Uncertainty Principles: Exact Signal Reconstruction from Highly Incomplete Frequency Information," *IEEE Transactions on Information Theory*, vol. 52, no. 2, pp. 489–509, Feb. 2006.

[12] ——, "Stable Signal Recovery from Incomplete and Inaccurate Measurements," *arXiv:math/0503066*, Dec. 2005, arXiv: math/0503066. [Online]. Available: http://arxiv.org/abs/math/0503066

[13] C. Eckart and G. Young, "The approximation of one matrix by another of lower rank," *Psychometrika*, vol. 1, no. 3, pp. 211–218, Sep. 1936. [Online]. Available: https://doi.org/10.1007/BF02288367

[14] J. Wright, A. Y. Yang, A. Ganesh, S. S. Sastry, and Y. Ma, "Robust Face Recognition via Sparse Representation," *IEEE Transactions on Pattern Analysis and Machine Intelligence*, vol. 31, no. 2, pp. 210–227, Feb. 2009.

[15] Z. Drmač and S. Gugercin, "A New Selection Operator for the Discrete Empirical Interpolation Method—Improved A Priori Error Bound and Extensions," *SIAM Journal on Scientific Computing*, vol. 38, no. 2, pp. A631–A648, Jan. 2016, publisher: Society for Industrial and Applied Mathematics. [Online]. Available: https://epubs.siam.org/doi/10.1137/15M1019271

[16] B. M. de Silva, K. Manohar, E. Clark, B. W. Brunton, S. L. Brunton, and J. N. Kutz, "PySensors: A Python Package for Sparse Sensor Placement," *arXiv:2102.13476 [cs, eess, math]*, Feb. 2021.